Excluded volume effects in the end-to-end distance of two-generation dendritic polymers: TTT and HH combs

Excluded volume effects in the end-to-end distance of two-generation dendritic polymers: TTT and HH combs

Marios Kosmas[1]**, Cooper Reid**[2] **and Marvin Bishop**[2]

[1] Chemistry Department, University of Ioannina, Ioannina, 45110, Greece
[2] Department of Mathematics/Computer Science, Manhattan College, Manhattan College Parkway, Riverdale, NY 10471, USA

E-mail: mkosmas@cc.uoi.gr and marvin.bishop@manhattan.edu

Abstract

Excluded volume effects in the end-to-end distances of two-generation dendritic polymers, with various numbers of branches and branch lengths, are determined by calculating the expansion factors of the branches to the order $\varepsilon = 4 - d$. The general solution correctly recovers known results of materials with fewer junctions and generations, such as star, brush and block co-polymers. This general solution also predicts the behaviors of three-junction TTT and HH polymers containing equal length branches. Pivot Monte Carlo simulations on the last two classes of polymers compare well with the first-order ε renormalization group results.

PACS numbers: 02.70.Uu, 05.10.Cc, 05.40.Jc, 36.20.Ey, 36.20.Hb

1. Introduction

Complex polymeric structures are important as nanomaterials because of their large surface area and many terminal groups. These two factors lead to enhanced reactivity. Big interior cavities make these polymers useful as carriers of small molecules. Since the permeability of the flexible polymeric structures can be altered by changing the thermodynamic conditions [1], these small molecules can be captured or released in a controlled manner.

The general polymer structure we are studying in this work is the one shown in figure 1. It is a first-generation dendritic polymer having as its zeroth interior generation a three-branch star with three different branches of lengths a, b and c, respectively. At the ends of each of the branches, a second exterior generation is formed by attaching another set of stars each with fa, fb or fc branches and branch lengths Na, Nb and Nc, respectively. Many interesting polymer structures can be obtained from this general form. When the values of c, b, Nc and Nb are 0,
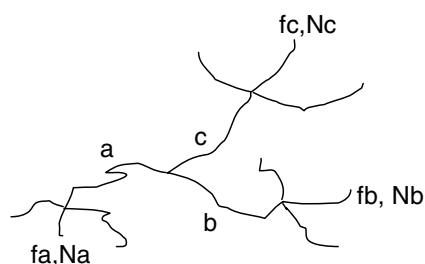
Figure 1. A dendritic polymer with two generations. The inert generation is a three-branch star with branch lengths *a*, *b* and *c*. Stars with *fa*, *fb* and *fc* extra branches (of lengths *Na*, *Nb* and *Nc*, respectively) emerge from the ends of the inert generation structure.
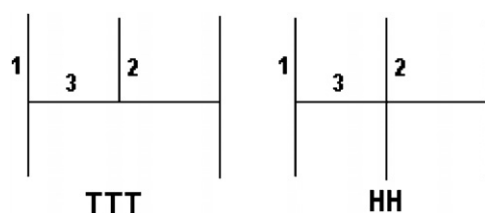

Figure 2. The TTT and HH polymers with equal branch length *N*. Branches 1 and 2 represent the side and central external branches, respectively, whereas branch 3 represents an internal branch.

and $a = 0$ or $a = Na$, one has a simple normal star with either *fa* or *fa* + 1 branches. A block co-polymer with lengths *a* and *b* for the two blocks is found when the values of *c*, *Nc*, *Na* and *Nb* are set to 0. Brush polymers with two-junction points are recovered when *c* and $Nc = 0$. Brush polymers behave as double stars made by joining the ends of two branches. The simplest of these are H-comb polymers which are determined from the general structure when *b* and $c = 0$, $Nc = 0$ and $fa = fb = 2$ while $fc = 0$. Also of special interest, because they are the two simplest three-junction polymers, are the TTT and HH polymers shown in figure 2. These polymers are built on double stars by incorporating linear chains at the junction point. These polymers can also easily be obtained from the general structure given in figure 1: TTT polymers when $c = 0$, $fa = fb = 2$ and $fc = 1$, or HH polymers when $fc = 2$.

In this paper we report on our renormalization group calculation for the general structure in figure 1, as well as Monte Carlo (MC) simulations of TTT and HH polymers with equal branch lengths, $a = b = Na = Nb = Nc = N$. The good agreement between the analytical results and the computational findings extends our understanding of the effects of large functionality on the conformational properties of complex macromolecules. The major property of interest in this work is the ratio, *r*, of the relative sizes of the internal and external branches. For the most general case of the structure of figure 1 there are six different kinds of branches, with lengths equal to *a*, *b* and *c* for the interior, and *Na*, *Nb* and *Nc* for the exterior branches respectively. The sizes of these various parts of the macromolecule reveal the effects on the specific parts of the chain and their contributions to the total macroscopic behavior. These sizes are easier to evaluate analytically than the radius of gyration. Moreover, the radius of gyration is the sum of all average distances between all pairs of chain points and only describes the overall size of the chain, without revealing the details of the interaction between different chain pieces.

2. Renormalization group calculation of the mean-square end-to-end distances of the branches

In the continuous line model of a chain counting the pair interactions between monomeric units corresponds to a double integration over all the points i and j of the positions of the units on the chain. According to the Gaussian model, the probability distribution P_o of any segment of length N' having its two ends separated by R' (when the spacing between individual chain units is of length $\ell = 1$) is given in the spatial dimension d by

$$P_o = \left(\frac{d}{2\pi}\right)^{d/2} \exp\left[-\frac{dR'^2}{2N'}\right]. \tag{1}$$

The mean-square end-to-end distance, $\langle R^2 \rangle$, of a specific part of the chain is equal to

$$\langle R^2 \rangle = \frac{\langle P_o \, \exp[-u \int di \int dj \delta[r(i) - r(j)]]R^2 \rangle}{\langle P_o \, \exp[-u \int di \int dj \delta[r(i) - r(j)]] \rangle}, \tag{2}$$

which to first order in the excluded volume parameter u for any polymeric structure is equivalent to the difference of the contributions from the numerator and denominator. It is equal to
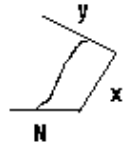
$$\langle R^2 \rangle = \langle R^2 \rangle_o - u \int di \int dj \left\{ \int dR \int dRx \left[\underset{\mathrm{Rx}}{\overset{0}{\underset{L}{\bigcirc}}} k \overset{N}{\underset{}{}} R \right] R^2 - \langle R^2 \rangle_o \bigcirc_L \right\} = N - u \int di \int dj \left\{ \int dR \int dRx \right.$$

$$\times \left(\frac{d}{2\pi k}\right)^{d/2} \left(\frac{d}{2\pi(L-k)}\right)^{d/2} \left(\frac{d}{2\pi(N-k)}\right)^{d/2} \mathrm{Exp}\left[-\frac{d}{2}\mathrm{Rx}^2\left(\frac{1}{k} + \frac{1}{L-k}\right)\right.$$

$$\left. -\frac{d}{2}\left(\mathrm{R} - \mathrm{Rx}\right)^2 \frac{1}{N-k}\right] \mathrm{R}^2 - \mathrm{N}\left(\frac{d}{2\pi L}\right)^{d/2} \right\} \tag{3}$$

where L is the length of the loop formed between the two interacting points i and j with a probability represented by the second diagram of equation (3), equal to $(d/2\pi L)^{d/2}$. The first diagram represents the chain segment of length N starting at an origin, passing through the vector position R_x on the loop, and ending at R. k is the length of the common part $0R_x$ of the segment $0R$ under study. After performing the R_x *and* R integrations of equation (3) in all space and absorbing a $(d/2\pi)^{d/2}$ term into u, one obtains an expression of the form [2]
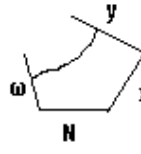
$$\langle R^2 \rangle = N + uF, \qquad F = \int di \int dj \frac{k^2}{L^{d/2+1}}. \tag{4}$$

The excluded volume parameter u expresses the intensity of the interactions. It is positive when there is a net repulsion and negative when there is a net attraction between the polymeric points. We have previously shown that first-order calculations at the critical dimensionality, $d = 4$, yield excluded volume effects to order $\varepsilon = 4 - d$ by means of the value of the excluded volume parameter $u^* = \varepsilon/16$ at the fixed point [3]. In the complex polymeric structure of figure 1 all interactions can be written in terms of three functions describing excluded volume effects in the same or between two different branches. At $d = 4$ the three necessary functions are given by

$$\overset{\frown}{\underset{\mathbf{N}}{}} = F_o(N) = \int_0^N di \int_0^N dj \frac{k^2}{L^3} = 2\int_0^N \frac{(N-L)}{L} dL = \lim_{\lambda \to 0} 2\int_\lambda^N \frac{(N-L)}{L} dL$$

$$= 2N\left[\ln\left(\frac{N}{\lambda}\right) - 1 + 0(\lambda/\mathrm{N})\right] \tag{5a}$$

3

$$= F_1[N, x, y] = 2\int_0^N di \int_0^y dj \frac{k^2}{L^3} = 2\int_0^N di \int_0^y dj \frac{i^2}{(i + j + x)^3}$$

$$= 2(x + y)\ln\left(\frac{N + x + y}{x + y}\right) - 2x\ln\left(\frac{N + x}{x}\right) + \frac{(x + y)^2}{N + x + y} - \frac{(x)^2}{N + x} - y \tag{5b}$$

$$= F_2[N, x, y, \omega] = 2\int_0^\omega di \int_0^y dj \frac{k^2}{L^3} = 2\int_0^\omega di \int_0^y dj \frac{N^2}{(i + j + N + x)^3}$$

$$= N^2\left[\frac{1}{N + x + y + \omega} - \frac{1}{N + x + y} - \frac{1}{N + x + \omega} + \frac{1}{N + x}\right]. \tag{5c}$$

Among these three functions only F_o represents intra-segmental excluded volume effects (equation (5a)). In this case $k = L$ and the use of the small length cutoff parameter λ is necessary for the existence of this excluded volume contribution and the determination of the known critical exponents. This is achieved by means of renormalization group theory which employs renormalized quantities like N/λ at the fixed point value $u^* = \varepsilon/16$, absorbing actually the cutoff parameter λ in the chain length N. At the fixed point, not only are proper exponents such as the exponent $\nu = \frac{1}{2} + \varepsilon/16$ produced at the infinite molecular weight limit but also other terms independent of N which still contribute to the values of the corresponding properties. In the ratios r evaluated below, the difference of the numerator and the denominator contributions in N cancels, leaving the remaining quantities to determine the effects of the parameters on the ratios. F_1 describes the excluded volume effects on a branch of length N from points on another branch of length y when the two branches are joined by a branch of length x. Finally, the effects from the interacting points of two different branches of lengths y and ω when they include the branch of length N are given by F_2 where the ω branch is joined to the first end of the N segment and the second y branch is at a distance x from the second end. The employment of the F functions is equivalent to the methods used earlier involving the values of all different diagrams. The recovery of previous results for special classes of macromolecules by the present work with the F functions, as shown in equations (7)–(10), proves the equivalence of the two procedures. Using these three functions, the mean-square end-to-end distances of the exterior branches have the following form:

$$\langle R_{Na}^2 \rangle = N_a + uF,$$
$$\begin{aligned} F = F_o(N_a) &+ (f_a - 1)F_1(N_a, 0, N_a) + F_1(N_a, 0, a) + F_1(N_a, a, b) \\ &+ F_1(N_a, a, c) + f_b F_1(N_a, a + b, N_b) + f_c F_1(N_a, a + c, N_c), \end{aligned} \tag{6a}$$

whereas the interior branches have the form

$$\langle R_a^2 \rangle = a + uF',$$
$$\begin{aligned} F' = F_o(a) &+ f_a F_1(a, 0, N_a) + F_1(a, 0, b) + F_1(a, 0, c) + f_b F_1(a, b, N_b) + f_c F_1(a, c, N_c) \\ &+ f_a F_2(a, 0, b, N_a) + f_a F_2(a, 0, c, N_a) + f_a f_b F_2(a, b, N_b, N_a) \\ &+ f_a f_c F_2(a, c, N_c, N_a). \end{aligned} \tag{6b}$$

The expressions of the a sub-dendron are symmetric to the interchange of the b and c indices as expected. The other mean-square end-to-end distances of the b and c sub-dendrons can be obtained from these expressions by a cyclic change of the letters.

Known results are easily recovered from these general expressions. The mean-square end-to-end distance of a single branch of a star with f branches, each of length N, is given by [4, 5]

$$\langle R^2 \rangle = N \left\{ 1 + 2u \left[\ln N - 1 + (f-1)\left(\ln 2 - \tfrac{1}{4} \right) \right] \right\}. \tag{7}$$

This expression can be obtained from equation (5) by either setting $f_a = f$, $N_a = N$ and all the other branch lengths to zero or using $N_a = a = N$, $f_a = f + 1$ with all the other branch lengths set to zero. The mean-square end-to-end distance of the a block of a block co-polymer molecule is equal to [6]

$$\langle R^2 \rangle = N_a \left\{ 1 + 2u \left[\ln Na - 1 + \frac{Nb}{Na} \ln \left(\frac{Na + Nb}{Nb} \right) - \frac{Nb}{2(Na + Nb)} \right] \right\}, \tag{8}$$

with a similar equation for the b block. This form can also be recovered from equation (5) by using the values of the parameters given in the introduction. The sizes of the branches of a brush polymer with two junctions of equal length N has been found [5] to be

$$\langle R_{Na}^2 \rangle = N \left\{ 1 + 2u \left[\ln(N) - 1 + (f_a - 1)\left(\ln 2 - \tfrac{1}{4} \right) + (f_b - 1)\left(2\ln 3 - 3\ln 2 - \tfrac{1}{12} \right) \right] \right\} \tag{9}$$

and

$$\langle R_a^2 \rangle = N \left\{ 1 + 2u \left[\ln(N) - 1 + (f_a + fb - 2)\left(\ln 2 - \frac{1}{4} \right) + \frac{(fa - 1)(f_b - 1)}{6} \right] \right\}. \tag{10}$$

These expressions as well as the special case of regular combs with three branches given in [2] can be found from equations (6).

The simplest structure for which the external and internal mean-square end-to-end distances can differ is the H polymer. This polymer has four external and one internal branch. One way to obtain a uniform (all branches of equal length N) H polymer from the general expression (6) is to put $a = Na = Nb = N$, $c = b = Nc = 0$ and $fa = fb = 2$ *with* $fc = 0$. The external and internal sizes can be predicted from equations (6*a*) and (6*b*). Realizing that the F's become zero when the length of an interacting part is zero, the following results for the external, $\langle R_e^2 \rangle$, and internal, $\langle R_i^2 \rangle$, mean-square end-to-end distances are found:

$$\langle R_e^2 \rangle = N + u[F_o(N) + 2F_1(N, 0, N) + 2F_1(N, N, N)] \tag{11a}$$

and

$$\langle R_i^2 \rangle = N + u[F_o(N) + 4F_1(N, 0, N) + 4F_2(N, 0, N, N)]. \tag{11b}$$

Evaluation of the F functions from equations (5) and employment of the fixed point value $u^* = \varepsilon/16$ yields

$$\langle R_e^2 \rangle = N\{1 + (\varepsilon/8)(\ln N + 4\ln 3 - 4\ln 2 - 5/3)\} \tag{12a}$$

and

$$\langle R_i^2 \rangle = N\{1 + (\varepsilon/8)(\ln N + 4\ln 2 - 4/3)\}. \tag{12b}$$

These equations reproduce equations (3.6) and (3.7) in [5]. The ratio of these two equations is equal to the difference of the two terms to order ε; the $\ln N$ dependence cancels and we obtain

$$r = \langle R_i^2 \rangle / \langle R_e^2 \rangle = 1 + (\varepsilon/8)(8\ln 2 - 4\ln 3 + 1/3). \tag{13}$$

When $d = 3$, $\varepsilon = 1$ and thus $r = 1.186$, whereas when $d = 2$, $\varepsilon = 2$ and $r = 1.371$. These renormalization group results compare very well with computer simulation. Gaunt *et al* [7] studied r in two-dimensional H polymers using both exact enumeration and an inverse restricted MC sampling technique. They found that the inner branch was more expanded than the outer branches and that $r = 1.36 \pm 0.04$. Bishop and Saltiel [8] employed Brownian

dynamics with a bead-spring model and found an r value of 1.34 ± 0.02. Three-dimensional lattice simulations by Lipson *et al* [9] reported the ratio for different lattice types: face-centered cubic 1.22 ± 0.03, body-centered cubic 1.22 ± 0.03, simple cubic 1.22 ± 0.03 and tetrahedral 1.21 ± 0.03. Kosmas *et al* [4] used MC on a simple cubic lattice to find that $r = 1.20 \pm 0.05$, and Bishop and Saltiel [10] found that $r = 1.15 \pm 0.08$. Shida *et al* [11] employed another MC algorithm to investigate this problem and determined that r was about 1.23.

The corresponding equations for TTT and HH polymers with equal branch lengths can be obtained from the general structure of figure 1 if we put $c = 0$, $N_a = N_b = N_c = N$, $f_a = 2$, $f_b = 2$ and $f_c = 1$ or 2 for the TTT or HH polymers, respectively. Three different kinds of branches are realized for these polymers which are denoted in figure 2 as follows: 1 (external), 2 (middle external) and 3 (internal) joining the two. By means of equation (6) we find for the mean-square end-to-end distances of the three different branches, in a TTT polymer, the expressions

$$\langle R_1^2 \rangle = N \left\{ 1 + \frac{\varepsilon}{16} [F_o(N) + 2F_1(N, 0, N) + 2F_1(N, N, N) + 2F_1(N, 2N, N)] \right\} \tag{14a}$$

$$\langle R_2^2 \rangle = N \left\{ 1 + \frac{\varepsilon}{16} [F_o(N) + 2F_1(N, 0, N) + 4F_1(N, N, N)] \right\} \tag{14b}$$

$$\langle R_3^2 \rangle = N \left\{ 1 + \frac{\varepsilon}{16} [F_o(N) + 4F_1(N, 0, N) + 2F_1(N, N, N) + 4F_2(N, 0, N, N) \right.$$
$$\left. + 4F_2(N, N, N, N)] \right\}. \tag{14c}$$

and for the HH case:

$$\langle R_1^2 \rangle = N \left\{ 1 + \frac{\varepsilon}{16} [F_o(N) + 2F_1(N, 0, N) + 3F_1(N, N, N) + 2F_1(N, 2N, N)] \right\} \tag{15a}$$

$$\langle R_2^2 \rangle = N \left\{ 1 + \frac{\varepsilon}{16} [F_o(N) + 3F_1(N, 0, N) + 4F_1(N, N, N)] \right\} \tag{15b}$$

$$\langle R_3^2 \rangle = N \left\{ 1 + \frac{\varepsilon}{16} [F_o(N) + 5F_1(N, 0, N) + 2F_1(N, N, N) \right.$$
$$\left. + 6F_2(N, 0, N, N) + 4F_2(N, N, N, N)] \right\}. \tag{15c}$$

By means of equation (5) the values of the F functions are found to be equal to

$$F_o(N) = 2N[\ln(N) - 1], \qquad F_1(N, 0, N) = N \left(\ln 2 - \frac{1}{2} \right),$$

$$F_1(N, N, N) = N \left(4 \ln 3 - 6 \ln 2 - \frac{1}{6} \right),$$

$$F_1(N, 2N, N) = N \left(-10 \ln 3 + 16 \ln 2 - \frac{1}{12} \right), \tag{16}$$

$$F_2(N, 0, N, N) = \frac{N}{3}, \qquad F_2(N, N, N, N) = \frac{N}{12}$$

so that the final results for these two special polymers are given by

$$\langle R_1^2 \rangle = N \left\{ 1 + \frac{\varepsilon}{8} \left[\ln N - 6 \ln 3 + 12 \ln 2 - \frac{7}{4} \right] \right\} = N \left\{ 1 + \frac{\varepsilon}{8} [\ln N - 0.02] \right\} \tag{17a}$$

$$\langle R_2^2 \rangle = N \left\{ 1 + \frac{\varepsilon}{8} \left[\ln N + 8\ln 3 - 10\ln 2 - \frac{11}{6} \right] \right\} = N \left\{ 1 + \frac{\varepsilon}{8} [\ln N + 0.02] \right\} \quad (17b)$$

$$\langle R_3^2 \rangle = N \left\{ 1 + \frac{\varepsilon}{8} \left[\ln N + 4\ln 3 - 2\ln 2 - \frac{8}{6} \right] \right\} = N \left\{ 1 + \frac{\varepsilon}{8} [\ln N + 1.67] \right\} \quad (17c)$$

for the TTT polymer and

$$\langle R_1^2 \rangle = N \left\{ 1 + \frac{\varepsilon}{8} \left[\ln N - 4\ln 3 + 9\ln 2 - \frac{11}{6} \right] \right\} = N \left\{ 1 + \frac{\varepsilon}{8} [\ln N + 0.01] \right\} \quad (18a)$$

$$\langle R_2^2 \rangle = N \left\{ 1 + \frac{\varepsilon}{8} \left[\ln N + 8\ln 3 - 9\ln 2 - \frac{25}{12} \right] \right\} = N \left\{ 1 + \frac{\varepsilon}{8} [\ln N + 0.47] \right\} \quad (18b)$$

$$\langle R_3^2 \rangle = N \left\{ 1 + \frac{\varepsilon}{8} \left[\ln N + 4\ln 3 - \ln 2 - \frac{5}{4} \right] \right\} = N \left\{ 1 + \frac{\varepsilon}{8} [\ln N + 2.45] \right\} \quad (18c)$$

for the HH polymer. These equations predict that $\langle R_1^2 \rangle < \langle R_2^2 \rangle < \langle R_3^2 \rangle$ for both shapes and that the $\langle R^2 \rangle$'s of HH polymers are larger than those of TTT polymers because of the interactions from the extra interacting branch in the HH polymer.

3. Pivot Monte Carlo simulations

Tangent hard sphere polymer models have been simulated using a Monte Carlo pivot [12] algorithm. Our polymer models are essentially the same as those previously employed by Zweier and Bishop [13] for H polymers. In these models all the atoms making up the monomeric polymer building blocks are grouped into a spherical 'bead'. The distance between two connected units is assumed to be a constant of magnitude one; e.g. adjacent beads are tangent. If m is the number of units in a branch, then the total number of units in a TTT polymer is $N = 7 * m + 1$, whereas a HH polymer has $N = 8 * m + 1$ units. We have simulated systems with N ranging from 211 to 701 or 241 to 881 in the case of TTT or HH polymers, respectively. In the TTT polymer, the center of the first-junction bead is assigned as the origin of the XYZ coordinate system. The polymer is initially started with each of its seven branches either horizontally or vertically directed from the junction beads. The first three branches extend vertically in the positive direction, vertically in the negative direction and horizontally in the positive direction from the first-junction bead, respectively. The third branch connects the first two junctions. The second junction has one vertical and one horizontal branch. The horizontal branch connects the second to the third junction. This junction in turn has two vertical branches. An HH polymer has the same initial structure for these seven branches but includes another vertical branch at the second junction (see figure 3).

The polymers are started in the *X–Y* plane. The beads are moved in continuous space by the pivot algorithm. First, a random number is used to select one of the beads as a 'pivot'. If the first-junction bead is chosen as the pivot, then one of the first three branches is randomly selected to be moved. Likewise, if the second-junction bead is selected, then either the third, fourth or fifth branches will be moved in the case of a TTT polymer, or the third, fourth, fifth or sixth branch will be moved for a HH polymer. In the case in which the third branch is chosen, depending upon which junction was selected, either the first and second branches, or the rest of the branches are also moved as a unit with the third branch. Similar movement rules apply for the third junction.

Once a set of beads has been selected to be moved, we generate three randomly chosen Euler angles and then move all selected beads in accordance with standard rotation equations
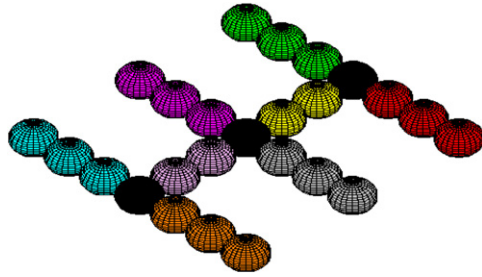
Figure 3. An HH polymer with 25 beads.

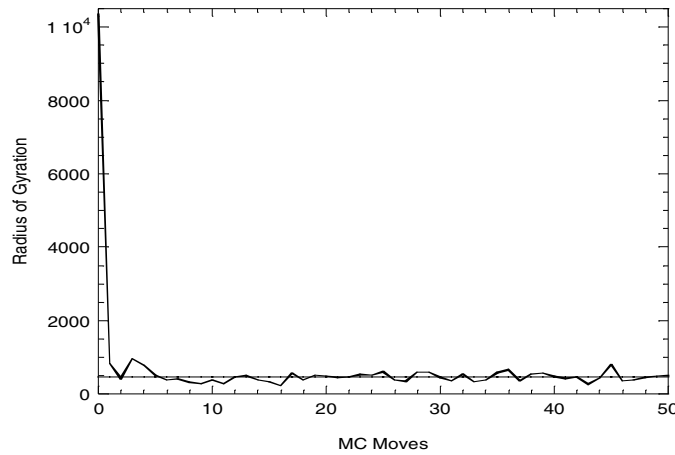(This figure is in colour only in the electronic version)

Figure 4. The relaxation of the radius of gyration of an 881-unit EV HH comb from its initial starting configuration.

[14]. If the pivot selected is a branch bead, then all the higher indexed beads on that branch are rotated about the pivot bead. In the excluded volume (EV) case the new trial configuration is accepted or rejected depending upon whether or not any beads overlap each other; no such testing is performed in the non-excluded volume (NEV) case.

These bead movement procedures generate one configuration. The process is continued for 5×10^6 moves but the first 1×10^6 moves are discarded before the averaging process begins. These discarded moves represent the equilibration of the initial arbitrary configuration. Data are collected at a spacing of 500 attempted pivot moves and the resulting random snapshots of polymer configurations are used for data analysis. Figure 4 shows the equilibration of an EV 881-unit HH polymer. The radius of gyration, S^2, which is a global property, is followed as a function of the number of attempted pivot MC moves. This quantity is computed by first determining the center of mass. If $\boldsymbol{R}_j$ denotes the three-dimensional position vector of the jth bead, then the center of mass coordinates, $\boldsymbol{R}_{\mathrm{CM}}$, of a given configuration are as follows:

$$\boldsymbol{R}_{\mathrm{CM}} = (1/N) \sum_{j=1}^{N} \boldsymbol{R}_j, \tag{19}$$

and S^2 is computed as

$$S^2 = (1/N) \sum_{j=1}^{N} (\boldsymbol{R}_j - \boldsymbol{R}_{\mathrm{CM}})^2. \tag{20}$$

Figure 4 demonstrates that the convergence toward the equilibrium state is rapid. The horizontal line is the average value, $\langle S^2 \rangle$, over the total equilibration phase of 2000 cycles with 500 moves each. Note that only the results for the first 50 cycles are plotted to emphasize the convergence. Since the EV 881-unit polymer is expected to require the most cycles in order to converge, the 2000 cycles employed in all of the simulations should be more than sufficient to attain the equilibrium state.

In the NEV case the acceptance ratio is 1 and all configurations are accepted. In the EV case the acceptance ratio ranged from 32 to 37% depending upon the polymer architecture and N. In order to obtain additional independent configurations and thus enhance the statistical quality of the data, 16 parallel runs employing different random number seeds were performed.

If $\boldsymbol{R}_0$ and $\boldsymbol{R}_e$ denote the position vectors of a junction and of the end bead in an attached branch, respectively, then the square of the end-to-end distance of that branch in a given configuration is given by

$$R^2 = (\boldsymbol{R}_0 - \boldsymbol{R}_e) \cdot (\boldsymbol{R}_0 - \boldsymbol{R}_e). \tag{21}$$

Each saved configuration is employed in the calculation. R^2 was then averaged over the total number of saved samples and the appropriate number of branches, to determine the values of the mean and the standard deviation from the mean, employing the usual equations [15].

4. Results

TTT and H polymers in the NEV and EV regimes have been simulated. Table 1 presents the end-to-end distance simulation results for all the systems investigated. The number in parenthesis denotes one standard deviation in the last displayed digits. The error bars are smaller in the case of external branches since there are more external branches to average over. Note that the squares of the end-to-end distance of branches of type 1 and 2 (see figure 2) have been averaged together. As expected, NEV polymers are much more compact than their EV counterpart because excluded volume effects cause the polymer units to avoid each other and thus expand the polymer.

It is well known that for large polymers, $\langle R^2 \rangle$ follows the scaling law [16]

$$\langle R^2 \rangle = C(N-1)^{2v}, \tag{22}$$

where the coefficient C is a model-dependent amplitude but the exponent, $2v$, is universal for a given d and universality class; $2v$ has the value of about 1.20 in three dimensions for EV polymers and the value of 1.00 in all dimensions for random walk, NEV systems.

Weighted nonlinear least-squares fits [15] to equation (21) using the $\langle R^2 \rangle$ data in table 1 gave the values for the exponent, $2v$, of 0.993 ± 0.001 for both NEV TTT and HH polymers. The corresponding EV systems had values of 1.208 ± 0.001 and 1.211 ± 0.001. Given that our largest branches have only about 100 units, our simulation data exponents agree reasonably well with the predicted values. Moreover, if one takes the large N limit in equations (17) and (18) the mean-square end-to-end distances will scale as $N^{1 + \varepsilon/8}$, predicting an exponent of 1.125.

The r-ratios have been calculated from the end-to-end distance data in table 1 and the errors in these quantities have been computed from the standard equation, relating the error in

Table 1. Simulation data for $\langle R^2 \rangle$.

	NEV		EV	
N	Internal	External	Internal	External
		TTT		
211	30.01 (3)	30.02 (4)	111.02 (9)	94.16 (9)
351	49.95 (11)	50.00 (6)	210.43 (21)	176.87 (9)
561	80.07 (12)	80.05 (8)	374.01 (47)	314.16 (26)
631	89.92 (20)	89.84 (8)	431.91 (50)	362.61 (37)
701	99.78 (10)	100.02 (9)	490.24 (42)	412.38 (39)
		HH		
241	29.98 (5)	30.00 (2)	117.50 (9)	95.42 (6)
401	49.86 (9)	49.96 (4)	222.26 (18)	179.38 (11)
561	69.90 (12)	70.02 (6)	335.91 (31)	270.72 (23)
721	89.90 (13)	89.95 (10)	457.58 (52)	367.55 (16)
881	109.69 (15)	110.15 (6)	583.98 (52)	468.12 (45)

Table 2. The ratio of internal to external end-to-end distances.

TTT-comb			HH-comb		
N	NEV	EV	N	NEV	EV
211	1.000 (2)	1.179 (1)	241	0.999 (2)	1.231 (2)
351	0.999 (3)	1.190 (1)	401	0.998 (2)	1.239 (1)
561	1.000 (2)	1.191 (3)	561	0.998 (2)	1.241 (2)
631	1.001 (2)	1.191 (2)	721	0.999 (2)	1.245 (2)
701	0.998 (1)	1.189 (2)	881	0.996 (1)	1.248 (2)

a ratio to the error in the numerator and the error in the denominator. The simulation *r*-ratios are listed in table 2.

The number in parenthesis denotes one standard deviation in the last displayed digit. It is clear that in the NEV case there is no difference between an internal and an external branch or between a TTT and HH polymer. If one examines polymers for which there are the same number of units in a branch, $m = 30$, 50 or 90, it is also clear that the interior branches of the HH polymer are more expanded than those of the TTT polymer because of the repulsions from the extra branch. The computer results are in accord with the renormalization group predictions. However, the computer results are for finite *N* whereas the theories are for infinite *N*. The scaling law is given by

$$r = r_\infty(1 - K/N^\Delta), \tag{23}$$

where r_∞ is the value of the *r*-ratio for infinite *N*, *K* is a constant and Δ is the finite scaling exponent. In the NEV regime Δ has a value of 1.0 and it is believed that for three-dimensional EV polymers [17] it has the value of 0.47. To determine the value of *r* as *N* approaches infinity, one plots *r* versus $1/N^\Delta$ so that when $N \to \infty$, $1/N^\Delta \to 0$. The *r* value for infinite *N* can thus be found by determining the intercept of this graph after fitting a weighted least-squares linear line in $1/N^\Delta$ to each set of data in the tables. The extrapolated *r*-ratios are found to be 0.998 ± 0.002 and 0.996 ± 0.002 for NEV TTT and HH polymers and 1.211 ± 0.003 and 1.267 ± 0.003 for corresponding EV polymers. Shida *et al* [11] found that EV HH polymers had an *r*-ratio value of about 1.29. The NEV systems, as expected, show no expansion effects. The

EV values compare well to RG predictions which are obtained from equations (17) and (18) when $d = 3$ ($\varepsilon = 1$). The predicted ratio between the internal branch 3 and the average of the other two, in TTT polymers is equal to

$$2\left\langle R_3^2 \right\rangle \big/ \left(\left\langle R_1^2 \right\rangle + \left\langle R_2^2 \right\rangle\right) = 1 + (\varepsilon/8)(1.67) \tag{24}$$

or 1.209. For the HH polymer the ratio is given by

$$2\left\langle R_3^2 \right\rangle \big/ \left(\left\langle R_1^2 \right\rangle + \left\langle R_2^2 \right\rangle\right) = 1 + (\varepsilon/8)(2.45 - 0.24) \tag{25}$$

or 1.276.

5. Conclusion

The mean-square end-to-end distances of a dendritic polymer with two generations and various numbers and lengths of branches are investigated. Pivot Monte Carlo calculations of continuum, tangent hard sphere models of the TTT and HH polymers have been used to explore both the ideal and excluded volume regimes. The computer results are found to be in good agreement with the first-order renormalization group results in $\varepsilon = 4 - d$. Interior branches are expanded more and branches of the HH polymer are larger than those of the TTT polymer because of the repulsions from the extra branch.

Acknowledgments

References

[1] Rangou S, Theodorakis P E, Gergidis L N, Avgeropoulos A, Efthymiopoulos P, Smyrnaios D, Kosmas M, Vlahos C and Giannopoulos Th 2007 *Polymer* **48** 652
     Efthymiopoulos P, Kosmas M, Vlahos C and Gergidis L 2007 *Macromolecules* **40** 9164
[2] Vlahos C H and Kosmas M K 1987 *J. Phys. A: Math. Gen.* **20** 1471
[3] Kosmas M K 1981 *J. Phys. A: Math. Gen.* **14** 931
[4] Miyake A and Freed K F 1983 *Macromolecules* **16** 1228
[5] Kosmas M K, Gaunt D and Whittington S G 1989 *J. Phys. A: Math. Gen.* **22** 5109
[6] Sdranis Y S and Kosmas M K 1991 *Macromolecules* **24** 1341
[7] Gaunt D S, Lipson J E G, Whittington S G and Wilkinson M K 1986 *J. Phys. A: Math. Gen.* **19** L811
[8] Bishop M and Saltiel C J 1992 *J. Chem. Phys.* **97** 1471
[9] Lipson J E G, Gaunt D S, Wilkinson M K and Whittington S G 1987 *Macromolecules* **20** 1861
[10] Bishop M and Saltiel C J 1993 *J. Chem. Phys.* **98** 1611
[11] Shide K, Ohno K and Kawazoe Y 2002 *J. Chem. Phys.* **116** 10938
[12] Madras N and Sokal A D 1988 *J. Stat. Phys.* **50** 109
[13] Zweier S and Bishop M 2009 *J. Chem. Phys.* **131** 116101
[14] Rubio A M and Freire J J 1985 *Macromolecules* **18** 2225
[15] Bevington P R 1969 *Data Reduction and Error Analysis for the Physical Sciences* (New York: McGraw-Hill)
[16] de Gennes P G 1979 *Scaling Concepts in Polymer Physics* (Ithaca, NY: Cornell University Press)
[17] Le Guillou J C and Zinn-Justin J 1980 *Phys. Rev.* B **121** 3976